



# Assessment of wind–damage relations for Norway using 36 years of daily insurance data

Ashbin Jaison<sup>1,3</sup>, Asgeir Sorteberg<sup>1,3</sup>, Clio Michel<sup>2</sup>, and Øyvind Breivik<sup>1,2</sup>

<sup>1</sup>Geophysical Institute, University of Bergen, Bergen, Norway

<sup>2</sup>Norwegian Meteorological Institute, Bergen, Norway

<sup>3</sup>Bjerknes Centre for Climate Research, Bergen, Norway

**Correspondence:** Ashbin Jaison (ashbin.jaison@uib.no)

Received: 13 November 2023 – Discussion started: 17 November 2023

Revised: 6 March 2024 – Accepted: 16 March 2024 – Published: 23 April 2024

**Abstract.** Extreme winds are by far the largest contributor to Norway’s insurance claims related to natural hazards. The predictive skills of four different damage functions are assessed for Norway at the municipality and national levels on daily and annual temporal scales using municipality-level insurance data and the high-resolution Norwegian hindcast (NORA3) wind speed data for the period 1985–2020. Special attention is given to extreme damaging events and occurrence probabilities of wind-speed-induced damage. Because of the complex topography of Norway and the resulting high heterogeneity of the population density, the wind speed is weighted with the population. The largest per capita losses and severe damage occur most frequently in the western municipalities of Norway, which are more exposed to incoming storms from the North Atlantic, whilst there are seldom any large losses further inland. There is no single damage function that outperforms others. However, a good agreement between the observed and estimated losses at municipality and national levels for a combination of damage functions suggests their usability in estimating severe damage associated with windstorms. Furthermore, the damage functions are able to successfully reconstruct the geographical pattern of losses caused by extreme windstorms with a high degree of correlation. From event occurrence probabilities, the present study devises a damage classifier that exhibits some skill at distinguishing between daily damaging and non-damaging events at the municipality level. While large-loss events are well captured, the skewness and zero inflation of the loss data greatly reduce the quality of both the damage functions and the classifier for moderate- and weak-loss events.

## 1 Introduction

Wind-related damage claims account for 56 % of Norway’s insurance payouts related to natural hazards from 1980 to 2017 and are by far the largest component of loss claims related to natural hazards (DSB Norway, 2019). They can affect all sectors from forests to marine and housing infrastructures (Jensen et al., 2010; Gardiner et al., 2013). However, a detailed investigation into the relationship between Norwegian windstorms and damage has so far not been conducted for Norway. A comparison of different proposed storm damage models has only been conducted in a few countries due to a lack of long and sufficiently homogeneous insurance claims data (Cole et al., 2010; Prahla et al., 2015). Determining the best storm damage model is important in order to make accurate predictions of future damage, whether it be in a few days (short-term forecast) or in many years (climate change range). In this paper, we investigate the relations between windstorms and their associated damage by analysing 36 years of daily insurance data on the municipality level and daily maximum wind speed data using a set of storm damage functions. Furthermore, we develop a probabilistic damage classifier that distinguishes between damaging and non-damaging wind speeds to help improve early warning systems.

Establishing robust windstorm–damage relations may help predict storm damage risk in the weather forecasting context (Merz et al., 2020), roughly estimate the storm impact directly after it occurred in order to better plan the emergency response (Welker et al., 2021) and evaluate the change in risk in the longer term in conjunction with climate change. More-

over, understanding the monetary risk involved in extreme wind events is crucial from the insurer's perspective in order to fix reasonable premiums and estimate portfolio risk. Several methods in the literature assess the risk associated with extreme wind events across various sectors such as agriculture, transport and energy at varying spatial resolutions (Gliksman et al., 2023). Storm damage functions are one such method which describes the mathematical relation between the intensity of a natural hazard, here the wind speed, and the monetary loss incurred due to the event. There are mainly two types of storm damage functions: (1) the storm-based approach, which links historical losses to wind speed information, and (2) the hazard-based approach, which, in addition, makes use of micro-scale information such as the vulnerability, exposure and value of the assets. However, as detailed information about the damage is often proprietary, the most common approach, also used in the present study, is the storm-based approach (Dorland et al., 1999; Klawa and Ulbrich, 2003; Prahel et al., 2012, 2015). These storm damage functions can also be split into deterministic and probabilistic types (Prahel et al., 2012). The deterministic damage functions do not estimate the uncertainty in the wind speed–loss relation, whereas the probabilistic damage functions assume a statistical distribution for the model error. To make the deterministic and probabilistic models comparable, estimates from deterministic models are treated as equivalent to the mean of the estimates from the probabilistic models.

Storm damage functions must be regionally fitted because they are highly dependent on local features. The number and spatial extent of the damage caused by extreme wind strongly depend on the exposure level of assets (Cardona et al., 2012), which is connected to demography and economy both changing over time due to a variety of reasons such as urbanisation, higher infrastructure standards and economic growth. Moreover, building types, building codes, differing insurance policies and claims settlement practices can also influence the performance of storm damage functions (Walker, 2011) especially if they are not locally fitted. Norway has a complex topography with mountains and valleys and a rugged coastline with many fjords, with a major share of the population living along the coasts and in the valleys (Simensen et al., 2021). Therefore, the population density is an important factor to take into account when establishing storm damage functions (Donat et al., 2011a).

A number of studies have investigated storm damage and risk in relation to residential structures and other insured losses, mainly for Europe and, more particularly, Germany, using various damage functions and local information. Dorland et al. (1999) suggested a deterministic damage function by which loss increases exponentially with wind speed such that a slight increase in storm intensity can cause a significant increase in economic damage in the Netherlands and northwestern Europe. Meanwhile, analysing annual insurance loss due to windstorms in Germany, Klawa and Ulbrich (2003) advocated for a cubic relationship between the de-

viation in wind speed from its 98th percentile and the loss. Donat et al. (2011b) estimated the losses by fitting the Klawa and Ulbrich (2003) damage function at the district level for Germany. Heneka and Ruck (2008) and Heneka and Hofherr (2011) applied a probabilistic damage function for Germany, which incorporates the extreme value theory in conjunction with a non-linear function. However, this probabilistic damage function requires both claim and loss ratios, which are not commonly shared data and which we lack for Norway. To estimate the daily and annual losses at the district levels in Germany, Prahel et al. (2012) proposed a power-law-based probabilistic damage function where loss is proportional to a power of wind speed. They found out that the exponents range between 8 and 12, thus highlighting the need to fit the functions locally. Welker et al. (2016) simulated the spatial pattern of losses associated with historical windstorms that happened in Switzerland using the asset amount and the vulnerability, the latter depending on the wind gust. The agreement between the simulated loss and the observed insurance loss was shown to be not only reasonable but also case-dependent. They pointed to the uncertainty not only in the input data, such as in the wind gust, but also in the estimation of the assets and vulnerability. More recently, Koks and Haer (2020) developed an open-source hazard-based model that uses publicly available hazard, exposure and vulnerability data, and the loss estimates can be treated as a baseline for further research. Using three different methods, Held et al. (2013) found a steady increase in the values associated with a 10-year return loss by the end of the twenty-first century when considering only German private houses. Schwierz et al. (2010) suggested that, with climate change and increased storm intensity, Norway can expect a 16 % increase in annual losses associated with windstorms. However, a recent study by Severino et al. (2023) indicated a significant decrease in winter storm damage over Norway.

In the following section, we introduce the insurance loss data and NORA3 hindcast wind speed data along with the different storm damage functions. In Sect. 3, the climatology of the extreme winds and damage is presented in addition to the modelling results. We summarise and discuss the results in Sect. 4.

## 2 Data and methods

### 2.1 Insurance loss data

We use daily insurance loss data, composed of the daily accumulated number of claims and monetary loss, from the Norwegian Natural Perils Pool for each of the 356 municipalities constituting Norway. The data span 36 years, from 1985 to 2020. The loss data distinguish losses by natural event types such as floods, landslides, storm surges and windstorms. The present study focuses on the damage associated with windstorms.

Natural peril insurance is a compulsory part of the fire insurance held by almost all households in Norway (Sandberg et al., 2020). Because of the Norwegian Natural Perils Pool act, all buildings and movable properties which are insured against fire damage are also insured against natural disasters. All insurance companies underwriting fire insurance in Norway are obliged to become members of the Norwegian Natural Perils Pool and archive their losses. The fraction of households having fire insurance has stayed relatively constant over the period of interest; thus, the effect of varying market penetrations is small. In many previous studies, the loss ratio and claim ratio, which are dimensionless, are used to model storm–damage relations (Huang et al., 2001; Held et al., 2013; Prahel et al., 2015; Welker et al., 2016). However, Norwegian insurance does not include the total insured value, which prevents us from using the loss and claim ratios in the present study.

For a long time series of loss data, it is necessary to account for inflation. To adjust for the effect of inflation, the insurance loss is modified using the official Norwegian consumer price index (CPI) at a fixed year (SSB Norway, 2023a). The base year for the CPI in Norway is 2015, which we also use here. As an example, the relative difference of loss after an inflation adjustment is +60 % for the 1992 New Year's Day Storm and +7 % for Cyclone Dagmar in 2011.

Changes in exposure are another key variable that determines the intensity of losses incurred. Many studies use population as a proxy for exposure (see e.g. Simpson et al., 2014). Statistics Norway publishes yearly population data at the municipality level, which go back to 1951 (SSB Norway, 2023b). To address the change in exposure to a certain extent, we compute the loss per person for each municipality by dividing the insurance loss data by the yearly population. Other factors, which may influence exposure, such as changing building standards and wealth distribution, are not accounted for in the present study.

A few extreme events have caused the majority of the total damage associated with windstorms. The five largest events were responsible for NOK 4.3 billion (Norwegian krone) in damages (2015 values), which represents 36 % of the total insurance loss from 1985 to 2020. The most damaging events and their associated losses are given in Table S1 in the Supplement. As expected from the more intense cyclones reaching Norway in winter rather than in summer (Hoskins and Hodges, 2019), the most extreme events occur between November and April. The presence of such extreme events brings skewness into the loss distribution, and the absence of losses on most days of the year makes loss data zero inflated (excess number of zeroes in the data). The distribution skewness and the zero inflation (Fig. S1 in the Supplement) in the loss data are challenging for conventional fitting methods, such as the least squares method or maximum likelihood method. Figure S1 highlights a record high number of claims in the years 1994; 2015; and, to a lesser extent, 2011. This

can be attributed to the storm of 1994, Cyclone Dagmar in 2011, and the Nina and Ole storms in 2015 (Table S1).

## 2.2 The wind speed data from the NORA3 hindcast

The high-resolution NORA3 hindcast covers the period 1979–2021 (and is being extended). The spatial resolution of NORA3 is 3 km × 3 km, and the surface variables are archived at an hourly resolution. The non-hydrostatic, convection-permitting model HARMONIE-AROME (Seity et al., 2011; Haakenstad et al., 2021; Haakenstad and Breivik, 2022) ingests surface observations through a simple surface analysis scheme and blends this with initial fields from ERA5 (Hersbach et al., 2020). Boundary conditions are also taken from ERA5. The data are publicly available on <https://thredds.met.no/thredds/catalog/nora3/catalog.html> (last access: 1 March 2024). The domain covers the North Sea, the Norwegian Sea, the Barents Sea, and Svalbard, and it is bounded by Finland to the east. The hindcast consists in a sequence of 9 h forecasts initialised at 00:00, 06:00, 12:00 and 18:00 UTC every day from 1985 to 2020, which comprised the 36 years available at the time of our analysis. Aggregating the 4–9 h lead times provides an hourly dataset from which we extract the daily maximum wind speed and gust. NORA3 only slightly underestimates the maximum observed wind speed (Haakenstad et al., 2021; Solbrekke et al., 2021) and its interquartile range for the 10 strongest windstorms that affected Norway between 2009 and 2018 (Haakenstad et al., 2021), outperforming both the earlier hydrostatic 10 km Norwegian hindcast archive (NORA10; Reistad et al., 2011) and the recent ERA5 reanalysis.

## 2.3 Municipality-level wind speeds

As the insurance loss is at the municipality level, we must estimate a municipality-relevant wind speed to apply the storm damage functions. A simple approach is to average the daily maximum wind speed over all grid points contained in a given municipality. However, to compensate for the complex topography and disparate demography of Norway, we calculate a population-weighted wind speed to remove extreme wind events occurring over mountains, lakes and other population-sparse regions. We make use of the gridded population data at 1 km × 1 km for Norway for the period 2001 to 2019 (<https://www.ssb.no/natur-og-miljo/geodata>, last access: 1 March 2024; Strand and Bloch, 2009). As it does not cover the whole period of the study, we compute the average of the population in each grid cell over the available period (2001–2019). Then, this averaged population is remapped on the same 3 km × 3 km grid as the NORA3 data. To achieve this, we assign each population grid cell to the nearest NORA3 grid cell. If more than one non-zero population grid cell corresponds to a NORA3 cell, we assign the sum of the population grid cells to the NORA3 grid cell. Finally, in order to have the wind speed at the municipal-

ity level, as are the insurance data, we take the population-weighted average of the daily maximum wind speed in each municipality. We repeat the process for the daily maximum wind gusts.

## 2.4 Storm-loss models

Storm damage functions connect the intensity of a storm event to the monetary damage caused by the storm. With the available historical data of insurance loss and wind speed, we apply the storm-based approach to fit several storm damage functions. The storm damage functions discussed here are macroscale statistical models calibrated at the municipality level. Our key objective is to compare and assess the quality of various proposed storm damage functions applied to our data. We employ three damage functions: the deterministic exponential model (Dorland et al., 1999; Huang et al., 2001; Murnane and Elsner, 2012), the deterministic model of Klawa and Ulbrich (2003), and the probabilistic function by Prah et al. (2012). In addition, we suggest a modified version of the Prah model to better simulate the very steep damage curves found in some Norwegian municipalities. All damage models are fitted to loss per person to ensure uniformity among the storm damage approaches and easier inter-comparison of models and parameters. Finally, we devise a simple ensemble mean of the estimates from the four damage functions listed above to check if it performs better than any of the four individual functions. In Sect. 2.4, we describe in detail the damage functions applied. From now on,  $L$  refers to the insurance loss,  $v$  to the weighted wind speeds and  $d$  to the damage function.

To fit and assess the skill of the storm damage models, we split the data into a testing and a training set. We assign the years from 1985–1989 and 2010–2012 to the testing part. The rest of the data from 1990–2009 and 2013–2020 are the training data. A necessary condition for splitting the data is that the training and testing data should have identical distributions. We split the data so that both the testing and training data include extreme storm events, with Cyclone Dagmar in the testing data and the New Year’s Day Storm in training data.

For robust storm–damage relations, extreme care should be taken while calibrating the damage functions. To make sure that the small losses, which are more frequent, are not better fitted than the high losses, which are much less frequent, we bin the loss data with respect to wind speeds to reduce the weight of low-loss events. Note that we do not perform binning for the Klawa damage function as the model is only suitable for high-loss events and inherently decreases the number of zero and low losses with the use of a high wind speed threshold. More about binning in individual models is explained in the following sections.

As many previous studies before (Donat et al., 2011b; Prah et al., 2012, 2015; Pardowitz et al., 2016), we choose to fit the storm damage functions at the municipality level. De-

spite the issue with a larger number of zero or low losses, this method is more meaningful and has the potential to be more accurate than doing fits using a country-averaged population-weighted wind speed. For example, the number of loss days when the population-weighted wind speed exceeds its 98th percentile is high along the Norwegian coast and low for further-inland regions (Fig. S2a). Moreover, there are many local factors influencing the damage, such as building rules and building types, that promote local fits of the storm damage functions. As a test, we pooled all municipalities together to perform the fits, but they did not show any improvement in the estimation of both municipal- and national-level losses (Fig. S3).

### 2.4.1 Exponential model

The exponential damage function assumes that loss increases exponentially with increasing wind speed (Dorland et al., 1999). It is a simple damage function with only two parameters to be estimated and is formulated as

$$d(v) = e^{\alpha(v-\beta)}, \quad (1)$$

where  $\alpha$  is the scale parameter and  $\beta$  is the location parameter. The loss is estimated from the damage function as  $L(v) = d(v)$ . The exponential model, by its shape, can be extended to low wind speeds that may cause low- to medium-size losses. To take advantage of this, we choose the 95th percentile of the population-weighted wind speed in each municipality as the threshold for the exponential model above which the aggregated losses represent 82 % of the national losses that occurred in the training period. Such a threshold ensures that the model accounts for low to medium losses while discarding the very small losses in the lower-loss spectrum. The associated loss values are split into 10 equally spaced bins with respect to the wind speeds and with a precondition that at least 5 loss days belong to each bin, as in Prah et al. (2015). Note that Fig. 1a only displays six bins because the four other bins do not include the minimum of 5 loss days required in each bin. The binned losses are log-transformed, and with the assumption of normality, the least squares method is employed to estimate the model parameters. Figure 1a shows the shape of the damage function with the red line. Although we only use the wind speed bins above the 95th percentile of the wind speed to calculate the fit, the obtained exponential model can also be applied to the wind speeds below the 95th percentile, and we can get loss estimates for those wind speeds as well, as shown in Fig. 1a (see the dashed red line).

### 2.4.2 Cubic excess over the threshold model

The damage function proposed by Klawa and Ulbrich (2003) suggests that the loss increases cubically for wind speeds beyond a certain threshold. The Klawa model was originally developed as a loss index for Germany to estimate annual

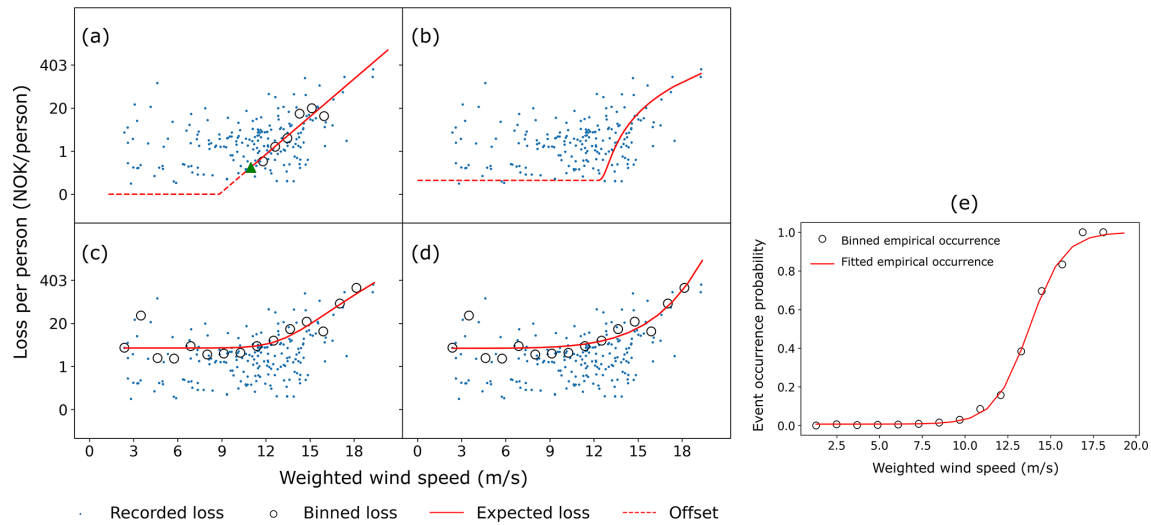


**Figure 1.** Shapes of the damage functions for an arbitrary municipality for (a) the exponential damage function where the green triangle denotes the loss corresponding to the 95th percentile of the wind speed and the dotted red line represents the loss estimates below the 95th percentile of the wind speed, (b) the cubic excess over the threshold damage function where the dotted red line represents the loss estimates below the 98th percentile of the wind speed, (c) the magnitude term in the probabilistic damage function by Prah, and (d) the magnitude term in the modified Prah probabilistic damage function. Panel (e) shows an example of the sigmoid function that estimates the probability of an event occurrence for an arbitrary municipality. The estimated parameters in this municipality are as follows:  $\gamma_0 = 0.99$ ,  $\gamma_1 = 0.99$  and  $\gamma_2 = 13.75$ . Note that the y axis for (a)–(d) is on a logarithmic scale and that the zero loss on the y axis is only for reference. The zero losses are not plotted.

national losses using German insurance data. Later, using the same insurance data, the damage function was calibrated by Donat et al. (2011b) for the German districts and by Pinto et al. (2012) for the affected areas of individual storm events. In the present study, we chose to calibrate the Klawa damage function with insurance loss at the municipality level similarly to Prah et al. (2015), who applied it at the district level to daily German insurance losses. This damage function takes the third power of wind speeds above the 98th percentile of the wind speed determined using the whole study period (1980–2020) scaled by the same 98th percentile of the wind speed as follows:

$$d(v) = \left( \frac{v - v_{98}}{v_{98}} \right)^3. \quad (2)$$

The loss is obtained by linear regressing the damage function as follows:

$$L(v) = \beta_0 + \beta_1 d(v). \quad (3)$$

The intercept term  $\beta_0$  in the fitted linear regression can be interpreted as the base loss, which is the loss estimate for all wind speeds below the 98th percentile. However, using this loss offset for all wind speeds below the 98th percentile does not address the randomness in the lower-loss spectrum. Figure 1b shows the model fit for this damage function (see the solid red and dashed red lines).  $\beta_1$  is the slope of the line. The two  $\beta$  parameters are obtained using a least squares regression method.

Several studies across Europe used the 98th percentile of the wind speed as a threshold for the Klawa damage function (Pinto et al., 2012; Karremann et al., 2014a, b). Ideally, the threshold for damaging wind should be locally chosen using statistically determined estimates; however, for simplicity, we have kept the frequently used 98th percentile. In Norway, 72 % of the insured losses are caused by wind speeds above the 98th percentile. As the Klawa model is not designed for low-loss cases, this is a fairly reasonable simplification. Note that if grid point wind speeds are chosen, this choice of percentile can be problematic for places with weak winds, such as southeastern Norway (see Fig. S4a). To alleviate this, Karremann et al. (2014b) and Little et al. (2023) suggested a  $9 \text{ m s}^{-1}$  fixed threshold for wind speeds causing damage in Norway. However, in our study, we do not need this  $9 \text{ m s}^{-1}$  threshold as we use the population-weighted averaged wind speeds, reducing the relative importance of grid cells with very low wind speeds and therefore avoiding the problem of the very low 98th percentile. Note that even wind speeds above the 98th percentile can be associated with no loss. Figure S2a shows that this often happens in the southern inland regions of Norway, where it contributes to the uncertainty in the loss estimation.

Here we weight the wind speeds with the population and aggregate it to the municipality-level resolution such that it corresponds to the loss data resolution. However, other studies, such as Pinto et al. (2007), weight the loss index and aggregate it to the district or national resolutions. As discussed

later in the paper, these two methods do not give very different results.

### 2.4.3 Probabilistic damage function by Prah1

The power-law-based probabilistic damage function by Prah1 et al. (2012) consists of a two-step fitting procedure: the first step is estimating the occurrence probability of damage for a given wind speed, and the second step is estimating the loss magnitude. For both steps, we use wind speed bins, and each bin must have at least 5 loss days, as Prah1 et al. (2015) did. We then fit the following sigmoid function to the binned wind speeds:

$$p(v) = 1 - \frac{\gamma_0}{1 + e^{\gamma_1(v-\gamma_2)}}, \quad (4)$$

where the parameter  $\gamma_1$  determines the steepness of the curve,  $\gamma_2$  is the wind speed threshold beyond which the curve gets steeper and  $\gamma_0$  determines the base probability of losses. Figure 1e shows the fit of the probability term (Eq. 4) of the damage function (see the red line). In addition, for a given wind speed  $v$ , the magnitude of the loss  $M$  for non-zero losses is estimated through a power-law-based function (Fig. 1c) and is related to the wind speed as follows:

$$M(v) = \sigma_0 + \left(\frac{v}{\sigma_2}\right)^{\sigma_1}, \quad (5)$$

where  $\sigma_2$  scales the wind speed,  $\sigma_1$  is the shape parameter and  $\sigma_0$  is the offset loss. The magnitude term is fitted on losses binned with respect to wind speeds.

The probability term makes use of the whole loss range, while the magnitude term only uses non-zero losses. The probability of damage and the magnitude of loss are treated as independent variables. The damage function is then the product of the probability and the magnitude of loss:

$$d(v) = p(v)M(v). \quad (6)$$

The damage function includes the assumption that the observed losses follow a log-normal distribution ( $M_{\text{obs}} \sim \text{LN}(\mu, \sigma)$ , where  $M_{\text{obs}}$  is the observed non-zero loss). Therefore, the expected loss for a given wind speed is

$$L = p(v)E(M(v)). \quad (7)$$

The probabilistic damage function by Prah1 has a complex fitting procedure with eight parameters to be estimated. We refer the readers to the work by Prah1 et al. (2015) to learn more about the parameters and fitting procedures of the model. The location ( $\mu$ ) and scale parameters ( $\sigma$ ) of the log-normal distribution are estimated using the maximum likelihood method, and the other parameters of the damage function are estimated with the least squares method.

### 2.4.4 Modified probabilistic damage function by Prah1

The rationale behind Prah1's damage function is that the loss increases steeply for extreme wind events (Fig. 1c). However, based on inspection of the quality of the fitted curves for very-high-loss events, we identified a need for an even steeper damage function for certain municipalities in Norway. As the deterministic exponential damage function increases sharply and shows good fits for some of the municipalities, we propose a modified version of the damage function by Prah1 that combines an exponential fit with the probabilistic aspect of the Prah1 model. The magnitude term in Eq. (5) of the Prah1 damage function is modified as follows:

$$M(v) = \sigma'_0 \exp \left[ \left( \frac{v}{\sigma'_2} \right)^{\sigma'_1} \right]. \quad (8)$$

The rest of the fitting procedure and assumptions are the same as for the Prah1 damage function. The shape of the magnitude term in Eq. (8) is displayed in Fig. 1d with the red line.

### 2.4.5 Ensemble mean method

The four damage functions presented above have different advantages and drawbacks. The ensemble mean is calculated as the arithmetic mean of the loss estimates of the four functions, with the hope to improve the overall accuracy, as proven for ensembles of numerical weather/climate simulations.

## 2.5 Damage classifier

A damage classifier labels a given wind speed as damaging or not and adds useful information for event preparedness. The probabilistic damage occurrence probability function in Eq. (4) gives us the opportunity to define a classifier that distinguishes between a damaging and a non-damaging event. To build a robust classifier, it is necessary to define the probability threshold that separates an event from a non-event. With non-event days outnumbering the event days (class imbalance), it is not straightforward to define the probability threshold as 0.5 or to evaluate the model performance for various probability thresholds on the basis of traditional receiver operating characteristic (ROC) curves and the corresponding area under the curves (AUC). To circumvent the problem of class imbalance in identifying the best probability threshold, we employ the precision recall curve and the associated  $F$  scores (cf. Sect. 2.6; Sokolova and Lapalme, 2009). Figure 2 shows the precision recall curve for an arbitrary municipality. The split point of the damage classifier corresponds to the probability threshold with the highest  $F$  score from the precision recall curve.

## 2.6 Model evaluation metrics

We evaluate the models' performance on the training and testing parts at the municipality level using the mean absolute

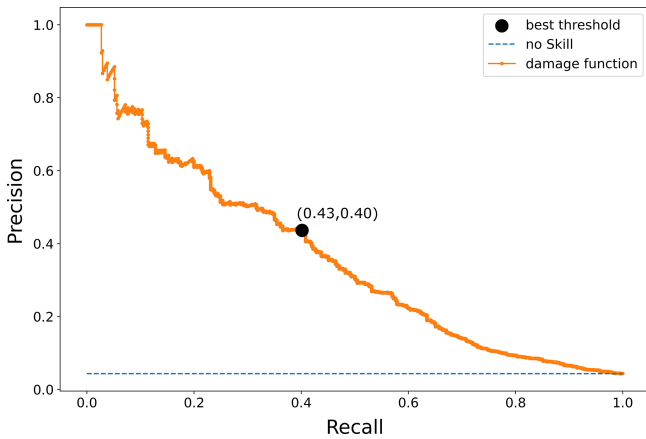


**Figure 2.** The orange line is the precision recall curve for an arbitrary municipality, the dashed blue line is the model with no skill, and the black dot corresponds to the point where the  $F$  score is maximum. In this example, the highest  $F$  score of 0.41 is achieved at the probability threshold of 0.30. The precision and recall are shown in brackets.

error (MAE) and coefficient of variation (CV). In addition, the predictive skill of the probabilistic function in the Prah1 damage function is evaluated using accuracy, recall, precision and  $F$  scores.

As its name indicates, the MAE is the mean of the absolute differences between the observations and the model fits and is formulated as

$$MAE = \frac{1}{n} \sum_{i=1}^n |y_i - \hat{y}_i|, \tag{9}$$

where  $y_i$  is the observed loss and  $\hat{y}_i$  is the estimated loss. A high MAE indicates a poor skill of the model. Another evaluation metric used here is the CV based on the root mean square error defined by Prah1 et al. (2015) as follows:

$$CV = \frac{1}{\bar{y}} \left( \frac{1}{n} \sum_{i=1}^n (y_i - \hat{y}_i)^2 \right)^{\frac{1}{2}}, \tag{10}$$

where  $\bar{y}$  is the mean of the observed loss. High values of the CV indicate large loss variability compared to the mean loss.

To quantify the classification skill of the damage classifier, we employ the precision, recall, accuracy and  $F$  scores, which are defined as follows:

- Precision is the proportion of correctly classified positive samples to the total number of samples classified as positive.
- Recall is the proportion of correctly classified positive samples to the total number of positive samples.
- Accuracy is the proportion of correctly classified samples to the total number of samples.

- The  $F$  score is, theoretically, defined as the harmonic mean of precision and recall. It indicates the balance between precision and recall. The  $F$  score ranges between 0 and 1, and the higher the  $F$  score, the better. We take advantage of the  $F$  scores to define the probability threshold for the damage classifier.

The binary damage classifier is optimised using the precision recall curve and associated  $F$  scores. The precision recall curve is obtained by calculating the precision and recall for all potential probability thresholds obtained from the observed occurrence probabilities. The  $F$  scores are computed for all points of the precision recall curve (i.e. all probability thresholds), and they simultaneously evaluate the ability of each probability threshold to minimise false positives and capture true positives. The probability threshold at which the  $F$  score is at its maximum is chosen as the split point for the event classifier.

The damage functions are sensitive to the extreme-loss observations, and the presence of a few extreme events can heavily alter the damage functions’ shape. Therefore, different training datasets may result in differing damage function fits. Cross-validation is an effective method to estimate the uncertainties involved in the choice of the testing and training data. We perform a 7-fold cross-validation by splitting the data into seven sets with each set of testing data having 5 consecutive years of data. So, in the first fold the testing period is 1985–1989 and the training period is 1990–2020. In the second fold, the testing period is 1990–1994 and the remaining years are in the training dataset, and so on.

### 3 Results

In this section, we analyse the spatial and temporal distribution of the insurance loss and compare the population-weighted daily maximum wind speed, the population-weighted daily maximum wind gust and the daily maximum wind speed at the municipality level. We then compare the different damage functions along with the modified Prah1 and ensemble mean models. However, considering the high degree of detail involved, we emphasise the following aspects: (1) daily losses at the municipality level, (2) top three extreme damaging wind events during the study period, (3) losses aggregated to the national level and (4) the probability function in Prah1 et al. (2012) as a classifier. Furthermore, we discuss the pitfalls of the loss data, wind data and storm damage functions.

#### 3.1 Overview of the losses from windstorms

The municipalities on the west coast of Norway experience higher losses per person, whereas there is hardly any loss further inland in southeastern Norway (Fig. S5a). Skewness and zero inflation are especially high for some municipalities in southeastern Norway where wind-related losses are rare.

This rarity of loss days greatly limits the performance of the damage functions.

The 10 most damaging windstorms, in terms of cost, that reached Norway during the study period occurred between October and March and mainly affected central and south-western Norway and, more marginally, Northern Norway (Table S1). An example of such a damaging storm is Cyclone Dagmar in 2011, which affected western Norway, causing more than NOK 1 billion in losses (Fig. S5b). The insurance losses caused by the 10 largest events are given in Table S1 and represent a total of NOK 5347 million, which is 44 % of the total losses due to windstorms between 1985 and 2020.

We find no significant temporal trends in the insurance losses caused by extreme winds. Trends in the loss time series should arise from inflation or changes in wealth distribution. However, the effect of inflation is nullified by adjusting the insurance losses with the consumer price index, and a change in wealth distribution is overlooked by the skewness in the losses. Therefore, the Mann–Kendall trend test that we conducted on the annual national losses (Fig. S6) fails to detect any significant trend in losses.

The choice of wind data has the potential to influence the performance of the damage functions (Prahl et al., 2015). Also, the 98th percentile of the wind speed is widely regarded as critical from a damage perspective (Klawns and Ulbrich, 2003; Schwierz et al., 2010; Donat et al., 2011a). Figure S4a shows that the west coast and Northern Norway experience high-magnitude wind events in comparison with southeastern municipalities. The 98th percentile of the population-weighted daily maximum wind speed exhibits a high correlation with the 98th percentile of the population-weighted daily wind gust (0.91) but a lower correlation with the 98th percentile of the unweighted daily maximum wind speed (0.61) (Fig. S4b). This difference can be attributed to the added information of population as weights for wind speed and emphasises the importance of accounting for demography.

From the damage perspective, the extreme damaging events are of topmost concern. For each municipality, we define the losses higher than the 99.7th percentile as the extreme-loss class and losses lying between the 98th and 99.7th percentiles as the high-loss class. The aggregated municipality losses in the extreme-loss class account for 85 % of the total national loss, while the high-loss class comprises 8 % of the total national loss. In each municipality, the extreme-loss class includes approximately 31 d in the training data and 9 d in the testing data (occurring on average around once a year). Segregation of losses into different classes helps to assess the performance of the damage functions for events of different severity.

By applying the different damage functions, we get daily fits of insurance loss for 10 227 d in the training dataset and predictions for 2922 d in the test dataset for every municipality in Norway.

### 3.2 Municipality-level loss estimations

To demonstrate the advantage of weighting wind speed with population, damage functions were also fitted with the original wind speed as the predictor variable. The prediction error in the test data shows that the population-weighted wind speed has a lower CV in 67 % of municipalities (see also Fig. S4c in the Supplement for the spatial distribution of where the original wind speed data perform better). From these results, we conclude that weighting wind speeds with population tends to improve the predictive performance of the damage functions. Therefore, from now on, we only use the population-weighted wind speeds when fitting the damage functions. The deterministic damage models, which are the Klawns and exponential damage functions, perform best in nearly two-thirds of the municipalities across all loss classes in terms of the MAE. Table 1 shows the performance of the four different damage functions defined in the methods section and of the ensemble mean for different loss classes. The deterministic models exhibit the smallest median MAE across all municipalities. Using the CV as the evaluation metric gives similar model performances as when using the MAE. The ensemble mean method does not massively outperform the competing models but tends to give better results than Prahl's two damage functions (Table 1). A map of the best model for each municipality exhibits a high heterogeneity with no obvious spatial pattern; that is, no model performs best in certain regions (Fig. S2b). Overall, our results suggest that the Klawns storm damage function is the best model for a large share of municipalities (37.6 %).

The spatial distribution of the MAE is not uniform but can be linked to the magnitude of the variance of losses, with municipalities with a large-loss variance having the largest MAEs (Fig. 3). In addition, the spatially heterogeneous distribution of losses (Fig. S5a) gives rise to spatially heterogeneous errors (Fig. 3b). The CV, which shows the extent of variability in losses in relation to the mean losses, exhibits a relatively heterogeneous structure (Fig. 3c). On the one hand, there is a tendency for a high CV in some inland municipalities of southeastern Norway, where the rarity of windstorms could be part of the reason. On the other hand, the northwest part of southern Norway also exhibits a high CV although windstorms are more frequent there (Fig. 3b).

Pooling all municipality-level population-weighted wind speeds together to perform the storm damage functions fits does not give better municipality-level loss estimations as expected because of local effects, such as a different population density and vulnerability. The most skilled model in each municipality is associated with a larger MAE than when the fit is performed at the municipality level (see Fig. S3a). This reduction in skill also occurs for the national-level losses (Fig. S3b).

Unlike previous studies (e.g. Pinto et al., 2007), which weighted the spatially aggregated loss index devised from cubic exceedance of wind speed above a sufficiently high



**Table 1.** Number of municipalities for which a model performs the best; that is, it has the smallest MAE as a function of the loss class, as defined in the text. The medians of the MAE and CV in all 356 municipalities are also given. Note that the results are based on the performances on the unseen testing data. Also, some municipalities are not evaluated in the high-loss class due to a lack of data.

Loss class	Damage function	Number of municipalities	MAE	CV
All loss days	Modified Prah1	32	31	245
	Prah1	46	28	238
	Klawa	134	22	212
	Exponential	91	24	218
	Ensemble mean	53	26	226
High-loss class	Modified Prah1	16	5	184
	Prah1	25	5	176
	Klawa	141	4	156
	Exponential	99	4	134
	Ensemble mean	39	5	161
Extreme-loss class	Modified Prah1	53	73	153
	Prah1	65	67	147
	Klawa	121	49	132
	Exponential	75	55	143
	Ensemble mean	42	66	143

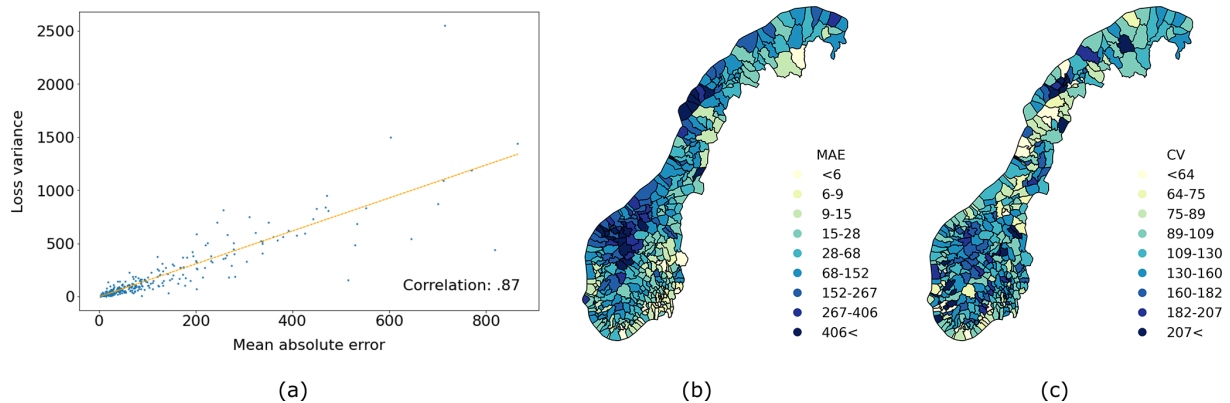


**Figure 3.** (a) Scatter plot of the loss variance against the smallest MAE for losses above the 99.7th percentile in the testing data where each dot represents a municipality. The orange line represents the linear trend obtained using a least squares regression with the correlation indicated in the bottom-right corner. (b) Map of the smallest MAE among the five models in the extreme-loss class fitted on the test data and (c) the corresponding coefficient of variation in the root mean square error. In (b) and (c), the legends have non-linear class boundaries at the 5th, 10th, 20th, 40th, 60th, 80th, 90th and 95th percentiles. Note that the results are based on the performances on the unseen testing data.

threshold (computed as in Eq. 2), we weight the wind speed with the population first and then aggregate it to a coarser resolution. We compare the Klawa damage function, as in Eq. (2), obtained from the proposed methodology with the alternative methodology employed in Pinto et al. (2007). We found both the damage estimates and their errors to be strongly correlated (Fig. S7a). An independent sample *t* test failed to find any significant differences between the mean of the MAEs from both methodologies. A detailed comparison can be found in the Supplement.

The 7-fold cross-validation reveals that the parameters in the storm damage functions obtained during the fitting step

depend on the choice of the training dataset. Moreover, the model evaluation metrics are highly dependent on the choice of the training dataset (see the range in Fig. S8a, b, d, e, g and h). However, independent of the training dataset, the Klawa and exponential models have the best skill in most of the municipalities (as also shown in Table 1) across the different loss classes (see Fig. S8c, f and i).

The fits of the four damage functions and of the probability term largely vary not only between models but also from municipality to municipality (Fig. S9). Figure S9a, c and d illustrate the variety among the fits for the exponential, Prah1 and modified Prah1 damage functions with very steep lines

for some municipalities and much flatter lines for others. Figure S9b highlights the fact that the Klawa damage function does not increase as steeply as the other models and the variability among the municipalities is smaller. Finally, Fig. S9e also shows that the sigmoid functions depicting the probability of damage occurrence have different shapes in different municipalities, with some curves not reaching a loss probability of 1 within the wind speed range represented. Note that the fit can lead to negative probabilities that we set to 0 afterwards.

### 3.3 Extreme damaging events

As extreme damaging windstorm events are of foremost importance, for example from the insurers' point of view, the ability of the damage functions to reproduce the damage associated with these events has to be assessed. To compare the estimated and observed losses caused by major storm events, we sum the loss within the date range as given by the Norwegian Natural Perils Pool in Table S1. Using only the model exhibiting the best performance, on the whole testing period, in each municipality, we manage to reproduce the spatial pattern of the damage for the three most damaging windstorm events (Fig. 4; see Fig. S10 for estimates from individual models for the three most damaging windstorm events and Table S2 for their corresponding correlations; also, Fig. S11 shows the spatial patterns of seven other damaging events as given in Table S1). Statistically significant spatial correlations between the observed and estimated losses reaffirm the suitability of the damage functions to estimate the economic impacts of extreme damaging events.

In the extreme-loss class, the probabilistic damage functions and the Klawa damage function perform best in a third of the municipalities each. The Klawa damage function also shows the smallest median error in the extreme-loss class, which is in agreement with previous comparison studies on storm damage functions over Germany (Prahl et al., 2015).

### 3.4 National-level loss

Aggregating the municipality-level loss observations and estimates yields a time series of daily national losses for each model, and we find an overestimation of low-magnitude losses as all damage functions are calibrated in favour of extreme losses (Fig. 5). Moreover, the models' estimates capture well the magnitude and temporal evolution of the observed annual losses at the national level, with a Spearman rank correlation coefficient of 0.84 (Fig. 6). Figure 6 also reveals that the losses in the extreme-loss class are slightly overestimated in the training period in years where extreme storm events have occurred, while there is an underestimation of loss in 2011 (part of the testing data) when Cyclone Dagmar occurred. The aggregated annual national-level losses for individual models are shown in Figs. S12 and S13. Figure S12 shows that the deterministic models

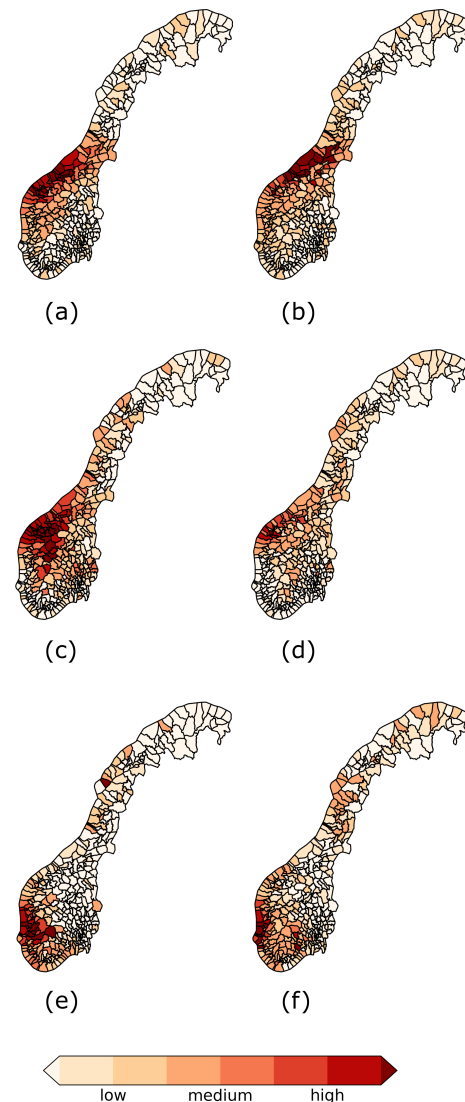


**Figure 4.** Spatial patterns of observed and estimated losses for the three most damaging events. Panels (a), (c) and (e) display the observed losses of the New Year's Day Storm, Cyclone Dagmar and Storm Nina. Panels (b), (d) and (f) are their respective estimates from the closest model to the observed loss in the testing period. The class boundaries of the colour bar are the 20th, 40th, 60th, 80th, 85th, 90th and 95th percentiles of the observed losses of their respective events. The spatial Spearman rank correlation between the observed and estimated losses of the New Year's Day Storm, Cyclone Dagmar and Storm Nina are 0.67, 0.58 and 0.62 respectively. For each storm, we sum all the loss days as given in Table S1.

are able to estimate well the losses in the extreme-loss class at the national level. The probabilistic models overestimate the losses in certain municipalities by a large margin, reducing the models' ability to estimate national-level losses (Fig. S13). While fitting the probabilistic damage functions, there are not enough extreme-loss observations in certain municipalities, which prevents us from requiring a minimum

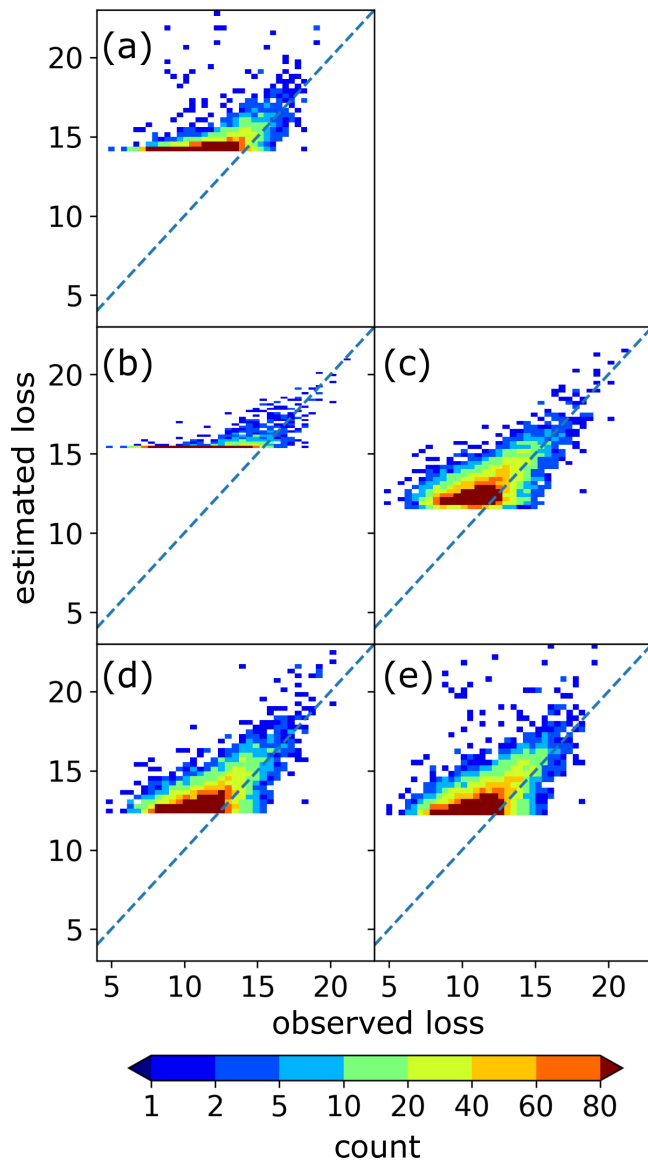


**Figure 5.** Observed and estimated daily losses (in NOK) on a log–log scale at the national level. Panels (a), (b), (c), (d) and (e) correspond to the ensemble mean method, the Klawa damage function, the exponential damage function, the Prahla damage function and the modified Prahla damage function respectively. The dashed blue lines represent the 1 : 1 line.

number of loss observations in each bin. This is one of the reasons for the very large differences between the observed and estimated losses for the probabilistic models.

### 3.5 Probability of damage occurrence

The damage classifier, devised here from the probability term in Prahla’s function (see Sect. 2.6), demonstrates some skill at predicting the most extreme events but struggles for the weaker events. It correctly predicts the top five extreme events (Table S3) for over 70 % of the municipalities. Even

though we try to address the excess number of zeroes with the precision recall curve, the classifier was only able to detect 20 %–40 % of the actual damaging events in most municipalities (see the number of municipalities in the [0.2, 0.4] interval in Fig. S14a) and zero events in around 15 % of the municipalities ( $\approx 50$  municipalities for the null true positive rate in Fig. S14a). Moreover, the false positive rate is small ( $< 4\%$ ) in all municipalities (Fig. S14b). Because of the noisy lower-loss regime, the calculated probability thresholds are low (Fig. S15) for most municipalities with values between 0.02 and 0.4 (median of 0.23; Fig. S15a). Only a few municipalities exhibit probability thresholds above 0.4, especially in southeastern Norway where damaging wind events are rare (Fig. S15b).

Although its skills are relatively poor, the damage classifier defined from event occurrence probabilities clearly outperforms a classifier that solely relies on wind speed. To demonstrate this, we define a damage classifier based on wind speed thresholds in which all wind speeds above the 98th percentile are labelled as damaging (as is done in the Klawa model). A comparison between these two classifiers shows a far higher accuracy for the classifier using the probability threshold (Fig. 7b) than for the classifier using the wind speed classifier threshold (Fig. 7a).

## 4 Conclusions

Windstorms are the natural hazard that makes up more than half of the monetary losses in Norway. The capability of four storm damage functions and their mean to reproduce the monetary losses associated with damaging wind events is evaluated for the complex topography and demography of Norway. The models’ ability to reproduce spatial loss patterns of extreme-loss events with a high degree of accuracy confirms the utility of both deterministic and probabilistic damage functions in estimating extreme-loss events. However, the relatively poor performance of the damage–no-damage classifier points towards the difficulty of developing an early warning system that also encompasses small-loss events. Our results confirm the importance of weighting wind speed with population, of locally fitting the storm damage functions and of using various damage functions to best estimate the losses from windstorms.

The deterministic Klawa model performs best in estimating extreme losses, and this result is consistent with previous studies, such as Prahla et al. (2015). In our study, the Klawa model also exhibits the smallest error in the entire loss range. However, the Klawa model’s inability to account for losses associated with wind speed below the 98th percentile greatly limits its applicability in the lower-loss range. The Prahla damage functions have the ability to model the whole loss range and show the smallest error in a third of the municipalities. The models’ performances suggest that relying on one single damage model may not be the best strategy

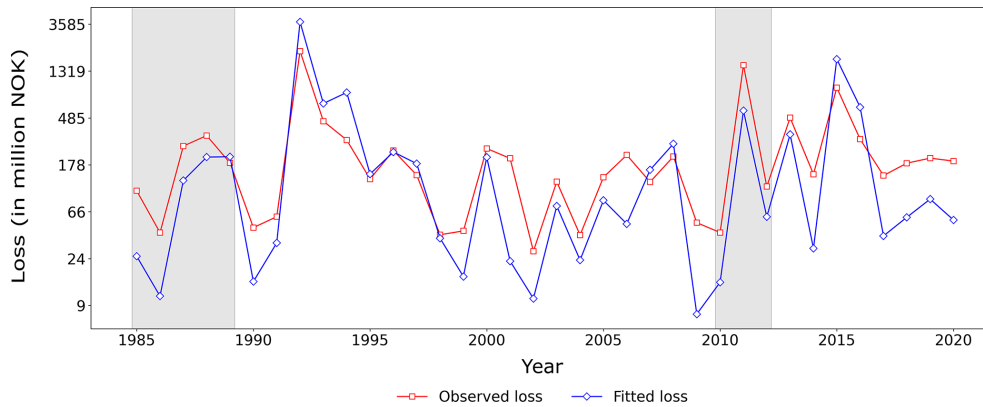


**Figure 6.** Annually aggregated national losses using only the loss days in the extreme-loss class from the insurance data (red line) along with the annual national loss estimates (blue line), which are the sum of each municipality’s best-performing-model estimate (see also Table 1). Note that the y axis is logarithmic and that the shaded region represents the testing period.

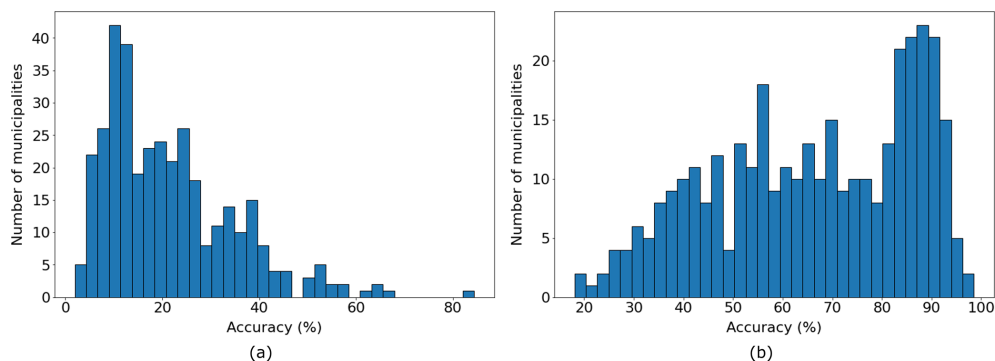


**Figure 7.** Distributions of (a) the accuracy of the damage classifier based on the 98th percentile of the wind speeds (median: 18 %) and of (b) the accuracy of the proposed damage classifier (Sect. 2.5) devised from the PrahL damage function (median: 68 %) for wind speeds above the 98th percentile, over all municipalities.

if all the municipalities in Norway are to be modelled. Due to the high spread in the fits of damage functions, the ensemble mean method mostly fails to outperform the individual models. Although the damage/no-damage classifier does very well at predicting extreme damaging events, more research is needed to propose a well-functioning damage classifier across all loss ranges.

Wind speed is the most common variable used to estimate storm damage. A drawback of this approach is that the same wind speed at the municipality-level resolution may cause small damage in some cases or no damage in most cases. Such inconsistencies occur mainly due to extremely local high wind gusts and incorrect reporting of damage. As a consequence, the lower end of the wind speed–damage relations becomes noisy, thus making it very difficult to model. To check how the wind gust from NORA3 compares to the wind speed, we performed the same population-weighting exercise with daily maximum wind gusts and found a high correlation (0.91) in the 98th percentiles calculated from wind speeds and wind gusts (Fig. S4b). With insurance data being at a coarser resolution than the wind gusts, which are very lo-

cal (a few hundred metres), it is difficult to get meaningful wind gust values at the municipality level because the impact of high values will be weakened by the population-weighted averaging step.

Due to the unavailability of the gridded population data for the earlier part (1985–1999) of our study period, we had to use a constant spatial distribution of the population to weight the wind speed at every grid point. Therefore, we cannot take into account the spatial change in population density, such as the spatial expansion of cities with time. This is a source of uncertainty in our storm-damage fits.

High-quality data on loss and wind speed are necessary for the calibration of damage functions. A long time series of loss data is desired to reduce uncertainties and increase accuracy of model fitting and predictions. However, loss information, as used in this study, is rarely available. In such cases, a general approach is to approximate the losses using the population of the respective regions and then quantifying the impact of windstorms (Donat et al., 2011a). In addition, there are open-source climate risk assessment models, such

as CLIMADA (Aznar-Siguan and Bresch, 2019), which can be coupled with loss data for damage estimation.

There are several limitations to the damage functions, including the inability of the models to account for the duration of the events and their tuning to model the extreme losses at the expense of the low losses. Furthermore, the randomness of the losses towards the lower-loss spectrum diminishes the damage classifier's predictive skill. There are also certain pitfalls in the insurance data, such as incorrect reporting of time, location and type of claims. Also, the slight underestimation of maximum wind speeds in NORA3 may affect the shape of the damage curves. A direct comparison between other studies that employ damage functions is not possible because the unit of loss in this study is NOK per person, while most other studies use the loss ratio (insured loss / total value of the insured assets) instead of the actual insured loss.

Applications of damage functions can range from impact-based forecasting of damage to damage assessment right after an event, as well as assessment of future losses in the context of climate change with an ensemble of wind–damage relations providing a measure of the uncertainty in the monetary loss amount. Previous studies suggest that with climate change the intensity of future windstorms may increase (see, for example, Priestley and Catto, 2022; Michel and Sorteberg, 2023). It would be worthwhile to assess the future changes in windstorm-induced losses using the damage functions discussed here and future wind speed projections. Impact-based forecasting, by which risks associated with a natural hazard are predicted in the short term, is gaining more popularity for climate risk management (Taylor et al., 2018; Zhang et al., 2019). The performance of these damage models, especially on the regional level, suggests their utility for impact-based forecasting. However, to use trained storm damage models on new data, one has to make sure that the distributions of the wind speed in the training dataset and the testing dataset are identical. To ensure this, statistical adjustment methods may be required. For forecasting purposes, an ideal starting point would be to apply a damage classifier to distinguish between damaging and non-damaging winds, as part of an early warning system, followed by a prediction of losses using a variety of damage functions. Also, from the risk-modelling perspective, coupling the damage functions with the asset exposure, i.e. information on infrastructures in addition to the population density, is a possible future direction.

*Code availability.* The codes of our analysis can be shared upon reasonable request.

*Data availability.* The NORA3 data are freely available at <https://thredds.met.no/thredds/projects/nora3.html> (Norwegian Meteorological Institute, 2021). The insurance data is proprietary, and the

dataset we use here cannot be shared. However, one can obtain some statistics at <https://nask.finansnorge.no> (Finance Norway, 2019).

*Supplement.* The supplement related to this article is available online at: <https://doi.org/10.5194/nhess-24-1341-2024-supplement>.

*Author contributions.* AJ handled the conceptualisation, analysis, visualisation, interpretation of results and drafting of the paper. AS conceived the idea and handled funding, supervision of the work and interpretation of results. CM handled the post-processing of the NORA3 data. ØB handled the supervision of the work and the funding. All authors contributed to drafting and reviewing the manuscript.

*Competing interests.* The contact author has declared that none of the authors has any competing interests.

*Disclaimer.* Publisher's note: Copernicus Publications remains neutral with regard to jurisdictional claims made in the text, published maps, institutional affiliations, or any other geographical representation in this paper. While Copernicus Publications makes every effort to include appropriate place names, the final responsibility lies with the authors.

*Acknowledgements.* We thank the Norwegian Natural Perils Pool and the Norwegian Meteorological Institute for providing the data. We are grateful to the two reviewers, who gave insightful comments on the manuscript, which helped to improve the quality of the manuscript.

*Financial support.* This research has been supported by the Research Council of Norway (grant no. 300608).

*Review statement.* This paper was edited by Joaquim G. Pinto and reviewed by two anonymous referees.

## References

- Aznar-Siguan, G. and Bresch, D. N.: CLIMADA v1: a global weather and climate risk assessment platform, *Geosci. Model Dev.*, 12, 3085–3097, <https://doi.org/10.5194/gmd-12-3085-2019>, 2019.
- Cardona, O. D., Van Aalst, M. K., Birkmann, J., Fordham, M., Mc Gregor, G., Rosa, P., Pulwarty, R. S., Schipper, E. L. F., and Sinh, B. T.: Determinants of risk: exposure and vulnerability, in: *Managing the risks of extreme events and disasters to advance climate change adaptation: special report of the intergovernmental panel on climate change*, 65–108, Cambridge University Press, <https://www.ipcc.ch/site/assets/uploads/2018/>

- 03/SREX-Chap2\_FINAL-1.pdf (last access: 1 March 2024), 2012.
- Cole, C. R., Macpherson, D. A., and McCullough, K. A.: A comparison of hurricane loss models, *Journal of Insurance Issues*, 33, 31–53, <http://www.jstor.org/stable/41946301> (last access: 1 March 2024), 2010.
- Donat, M. G., Leckebusch, G. C., Wild, S., and Ulbrich, U.: Future changes in European winter storm losses and extreme wind speeds inferred from GCM and RCM multi-model simulations, *Nat. Hazards Earth Syst. Sci.*, 11, 1351–1370, <https://doi.org/10.5194/nhess-11-1351-2011>, 2011a.
- Donat, M. G., Pardowitz, T., Leckebusch, G. C., Ulbrich, U., and Burghoff, O.: High-resolution refinement of a storm loss model and estimation of return periods of loss-intensive storms over Germany, *Nat. Hazards Earth Syst. Sci.*, 11, 2821–2833, <https://doi.org/10.5194/nhess-11-2821-2011>, 2011b.
- Dorland, C., Tol, R. S., and Palutikof, J. P.: Vulnerability of the Netherlands and Northwest Europe to storm damage under climate change, *Climatic change*, 43, 513–535, <https://doi.org/10.1023/A:1005492126814>, 1999.
- DSB Norway: Analyses of Crisis Scenarios 2019, [https://www.dsb.no/globalassets/dokumenter/rapporter/p2001636\\_aks\\_2019\\_eng.pdf](https://www.dsb.no/globalassets/dokumenter/rapporter/p2001636_aks_2019_eng.pdf) (last access: 1 March 2024), 2019.
- Finance Norway: <https://nask.finansnorge.no> (last access: 1 March 2024), 2019.
- Gardiner, B., Schuck, A. R. T., Schelhaas, M.-J., Orazio, C., Blennow, K., and Nicoll, B.: Living with storm damage to forests, vol. 3, European Forest Institute Joensuu, [https://efi.int/sites/default/files/files/publication-bank/2018/efi\\_wsctu3\\_2013.pdf](https://efi.int/sites/default/files/files/publication-bank/2018/efi_wsctu3_2013.pdf) (last access: 1 March 2024), 2013.
- Gliksman, D., Averbeck, P., Becker, N., Gardiner, B., Goldberg, V., Grieger, J., Handorf, D., Haustein, K., Karwat, A., Knutzen, F., Lentink, H. S., Lorenz, R., Niermann, D., Pinto, J. G., Queck, R., Ziemann, A., and Franzke, C. L. E.: Review article: A European perspective on wind and storm damage – from the meteorological background to index-based approaches to assess impacts, *Nat. Hazards Earth Syst. Sci.*, 23, 2171–2201, <https://doi.org/10.5194/nhess-23-2171-2023>, 2023.
- Haakenstad, H. and Breivik, Ø.: NORA3 Part II: Precipitation and temperature statistics in complex terrain modeled with a non-hydrostatic model, *J. Appl. Meteorol. Clim.*, 61, 1549–1572, <https://doi.org/10.1175/JAMC-D-22-0005.1>, 2022.
- Haakenstad, H., Breivik, Ø., Furevik, B. R., Reistad, M., Bohlinger, P., and Aarnes, O. J.: NORA3: A Nonhydrostatic high-resolution hindcast of the North Sea, the Norwegian Sea, and the Barents Sea, *J. Appl. Meteorol.*, 60, 1443–1464, <https://doi.org/10.1175/JAMC-D-21-0029.1>, 2021.
- Held, H., Gerstengarbe, F.-W., Pardowitz, T., Pinto, J. G., Ulbrich, U., Born, K., Donat, M. G., Karremann, M. K., Leckebusch, G. C., Ludwig, P., Nissen, K. M., Österle, H., Prah, B. F., Werner, P. C., Befart, D. J., and Burghoff, O.: Projections of global warming-induced impacts on winter storm losses in the German private household sector, *Climatic Change*, 121, 195–207, <https://doi.org/10.1007/s10584-013-0872-7>, 2013.
- Heneka, P. and Hofherr, T.: Probabilistic winter storm risk assessment for residential buildings in Germany, *Nat. Hazards*, 56, 815–831, <https://doi.org/10.1007/s11069-010-9593-7>, 2011.
- Heneka, P. and Ruck, B.: A damage model for the assessment of storm damage to buildings, *Eng. Struct.*, 30, 3603–3609, <https://doi.org/10.1016/j.engstruct.2008.06.005>, 2008.
- Hersbach, H., Bell, B., Berrisford, P., Hirahara, S., Horányi, A., noz Sabater, J. M., Nicolas, J., Peubey, C., Radu, R., Schepers, D., Simmons, A., Soci, C., Abdalla, S., Abellan, X., Balsamo, G., Bechtold, P., Biavati, G., Bidlot, J., Bonavita, M., Chiara, G. D., Dahlgren, P., Dee, D., Diamantakis, M., Dragani, R., Flemming, J., Forbes, R., Fuentes, M., Geer, A., Haimberger, L., Healy, S., Hogan, R. J., Hólm, E., Janisková, M., Keeley, S., Laloyaux, P., Lopez, P., Lupu, C., Radnoti, G., de Rosnay, P., Rozum, I., Vamborg, F., Villaume, S., and Thépaut, J.-N.: The ERA5 global reanalysis, *Q. J. Roy. Meteor. Soc.*, 146, 1999–2049, <https://doi.org/10.1002/qj.3803>, 2020.
- Hoskins, B. and Hodges, K.: The annual cycle of Northern Hemisphere storm tracks. Part I: Seasons, *J. Climate*, 32, 1743–1760, <https://doi.org/10.1175/JCLI-D-17-0870.1>, 2019.
- Huang, Z., Rosowsky, D. V., and Sparks, P. R.: Long-term hurricane risk assessment and expected damage to residential structures, *Reliab. Eng. Syst. Safe.*, 74, 239–249, [https://doi.org/10.1016/S0951-8320\(01\)00086-2](https://doi.org/10.1016/S0951-8320(01)00086-2), 2001.
- Jensen, Ø., Dempster, T., Thorstad, E., Uglem, I., and Fredheim, A.: Escapes of fishes from Norwegian sea-cage aquaculture: causes, consequences and prevention, *Aquaculture Env. Interac.*, 1, 71–83, <https://doi.org/10.3354/aei00008>, 2010.
- Karremann, M. K., Pinto, J. G., von Bomhard, P. J., and Klawa, M.: On the clustering of winter storm loss events over Germany, *Nat. Hazards Earth Syst. Sci.*, 14, 2041–2052, <https://doi.org/10.5194/nhess-14-2041-2014>, 2014a.
- Karremann, M. K., Pinto, J. G., Reyers, M., and Klawa, M.: Return periods of losses associated with European windstorm series in a changing climate, *Environ. Res. Lett.*, 9, 124016, <https://doi.org/10.1088/1748-9326/9/12/124016>, 2014b.
- Klawa, M. and Ulbrich, U.: A model for the estimation of storm losses and the identification of severe winter storms in Germany, *Nat. Hazards Earth Syst. Sci.*, 3, 725–732, <https://doi.org/10.5194/nhess-3-725-2003>, 2003.
- Koks, E. and Haer, T.: A high-resolution wind damage model for Europe, *Sci. Rep.*, 10, 1–11, <https://doi.org/10.1038/s41598-020-63580-w>, 2020.
- Little, A. S., Priestley, M. D., and Catto, J. L.: Future increased risk from extratropical windstorms in northern Europe, *Nat. Commun.*, 14, 4434, <https://doi.org/10.1038/s41467-023-40102-6>, 2023.
- Merz, B., Kuhlicke, C., Kunz, M., Pittore, M., Babeyko, A., Bresch, D. N., Domeisen, D. I., Feser, F., Koszalka, I., Kreibich, H., Pantillon, F., Parolai, S., Pinto, J. G., Punge, H. J., Rivalta, E., Schröter, K., Strehlow, K., Weisse, R., and Wulpst, A.: Impact forecasting to support emergency management of natural hazards, *Rev. Geophys.*, 58, e2020RG000704, <https://doi.org/10.1029/2020RG000704>, 2020.
- Michel, C. and Sorteberg, A.: Future Projections of EURO-CORDEX Raw and Bias-Corrected Daily Maximum Wind Speeds Over Scandinavia, *J. Geophys. Res.-Atmos.*, 128, e2022JD037953, <https://doi.org/10.1029/2022JD037953>, 2023.
- Murnane, R. J. and Elsner, J. B.: Maximum wind speeds and US hurricane losses, *Geophys. Res. Lett.*, 39, L16707, <https://doi.org/10.1029/2012GL052740>, 2012.

- Norwegian Meteorological Institute: NORA3 3-km Norwegian Reanalysis, <https://thredds.met.no/thredds/projects/nora3.html> (last access: 1 March 2024), 2021.
- Pardowitz, T., Osinski, R., Kruschke, T., and Ulbrich, U.: An analysis of uncertainties and skill in forecasts of winter storm losses, *Nat. Hazards Earth Syst. Sci.*, 16, 2391–2402, <https://doi.org/10.5194/nhess-16-2391-2016>, 2016.
- Pinto, J. G., Fröhlich, E. L., Leckebusch, G. C., and Ulbrich, U.: Changing European storm loss potentials under modified climate conditions according to ensemble simulations of the ECHAM5/MPI-OM1 GCM, *Nat. Hazards Earth Syst. Sci.*, 7, 165–175, <https://doi.org/10.5194/nhess-7-165-2007>, 2007.
- Pinto, J. G., Karremann, M. K., Born, K., Della-Marta, P. M., and Klawns, M.: Loss potentials associated with European windstorms under future climate conditions, *Clim. Res.*, 54, 1–20, <https://doi.org/10.3354/cr01111>, 2012.
- Prahl, B., Rybski, D., Kropp, J., Burghoff, O., and Held, H.: Applying stochastic small-scale damage functions to German winter storms, *Geophys. Res. Lett.*, 39, L06806, <https://doi.org/10.1029/2012GL050961>, 2012.
- Prahl, B. F., Rybski, D., Burghoff, O., and Kropp, J. P.: Comparison of storm damage functions and their performance, *Nat. Hazards Earth Syst. Sci.*, 15, 769–788, <https://doi.org/10.5194/nhess-15-769-2015>, 2015.
- Priestley, M. D. K. and Catto, J. L.: Future changes in the extratropical storm tracks and cyclone intensity, wind speed, and structure, *Weather Clim. Dynam.*, 3, 337–360, <https://doi.org/10.5194/wcd-3-337-2022>, 2022.
- Reistad, M., Breivik, Ø., Haakenstad, H., Aarnes, O. J., Furevik, B. R., and Bidlot, J.-R.: A high-resolution hindcast of wind and waves for the North Sea, the Norwegian Sea, and the Barents Sea, *J. Geophys. Res.-Oceans*, 116, C05019, <https://doi.org/10.1029/2010JC006402>, 2011.
- Sandberg, E., Økland, A., and Tyholt, I. L.: Natural perils insurance and compensation arrangements in six countries, <https://hdl.handle.net/11250/2659936> (last access: 1 March 2024), 2020.
- Schwierz, C., Köllner-Heck, P., Zenklusen Mutter, E., Bresch, D. N., Vidale, P.-L., Wild, M., and Schär, C.: Modelling European winter wind storm losses in current and future climate, *Climatic Change*, 101, 485–514, <https://doi.org/10.1007/s10584-009-9712-1>, 2010.
- Seity, Y., Brousseau, P., Malardel, S., Hello, G., Benard, P., Bouttier, F., Lac, C., and Masson, V.: The AROME-France Convective-Scale Operational Model, *Mon. Weather Rev.*, 139, 976–991, <https://doi.org/10.1175/2010MWR3425.1>, 2011.
- Severino, L. G., Kropf, C. M., Afargan-Gerstman, H., Fairless, C., de Vries, A. J., Domeisen, D. I. V., and Bresch, D. N.: Projections and uncertainties of future winter windstorm damage in Europe, *EGUsphere* [preprint], <https://doi.org/10.5194/egusphere-2023-205>, 2023.
- Simensen, T., Erikstad, L., and Halvorsen, R.: Diversity and distribution of landscape types in Norway, *Norsk Geogr. Tidsskr.*, 75, 79–100, <https://doi.org/10.1080/00291951.2021.1892177>, 2021.
- Simpson, A., Murnane, R., Saito, K., Phillips, E., Reid, R., and Himmelfarb, A.: Understanding risk in an evolving world: emerging best practices in natural disaster risk assessment, Global Facility for Disaster Reduction and Recovery, The World Bank, UN International Strategy for Disaster Reduction, Washington, DC, [https://www.gfdrr.org/sites/default/files/publication/Understanding\\_Risk-Web\\_Version-rev\\_1.8.0.pdf](https://www.gfdrr.org/sites/default/files/publication/Understanding_Risk-Web_Version-rev_1.8.0.pdf) (last access: 1 March 2024), 2014.
- Sokolova, M. and Lapalme, G.: A systematic analysis of performance measures for classification tasks, *Inform. Process. Manag.*, 45, 427–437, <https://doi.org/10.1016/j.ipm.2009.03.002>, 2009.
- Solbrekke, I. M., Sorteberg, A., and Haakenstad, H.: The 3 km Norwegian reanalysis (NORA3) – a validation of offshore wind resources in the North Sea and the Norwegian Sea, *Wind Energ. Sci.*, 6, 1501–1519, <https://doi.org/10.5194/wes-6-1501-2021>, 2021.
- SSB Norway: Consumer price index, <https://www.ssb.no/en/priser-og-prisindekser/konsumpriser/statistikk/konsumprisindeksen> (last access: 1 March 2024), 2023a.
- SSB Norway: Population 1 January and population changes during the calendar year (M) 1951–2023, <https://www.ssb.no/en/statbank/table/06913/> (last access: 1 March 2024), 2023b.
- Strand, G.-H. and Bloch, V. H.: Statistical grids for Norway, 9, [https://www.ssb.no/a/english/publikasjoner/pdf/doc\\_200909\\_en/doc\\_200909\\_en.pdf](https://www.ssb.no/a/english/publikasjoner/pdf/doc_200909_en/doc_200909_en.pdf) (last access: 1 March 2024), 2009.
- Taylor, A. L., Kox, T., and Johnston, D.: Communicating high impact weather: Improving warnings and decision making processes, *Int. J. Disast. Risk Re.*, 30, 1–4, <https://doi.org/10.1016/j.ijdr.2018.04.002>, 2018.
- Walker, G. R.: Modelling the vulnerability of buildings to wind – a review, *Can. J. Civil Eng.*, 38, 1031–1039, 2011.
- Welker, C., Martius, O., Stucki, P., Bresch, D., Dierer, S., and Brönnimann, S.: Modelling economic losses of historic and present-day high-impact winter windstorms in Switzerland, *Tellus A*, 68, 29546, <https://doi.org/10.3402/tellusa.v68.29546>, 2016.
- Welker, C., Rösli, T., and Bresch, D. N.: Comparing an insurer’s perspective on building damages with modelled damages from pan-European winter windstorm event sets: a case study from Zurich, Switzerland, *Nat. Hazards Earth Syst. Sci.*, 21, 279–299, <https://doi.org/10.5194/nhess-21-279-2021>, 2021.
- Zhang, Q., Li, L., Ebert, B., Golding, B., Johnston, D., Mills, B., Panchuk, S., Potter, S., Riemer, M., Sun, J., Taylor, A., Jones, S., Ruth, P., and Keller, J.: Increasing the value of weather-related warnings, *Sci. Bull.*, 64, 647–649, <https://doi.org/10.1016/j.scib.2019.04.003>, 2019.